

The Curious Problem of the Normal Inverse Mean *

Soham Ghosh¹, Uttaran Chatterjee², Jyotishka Datta³

October 29, 2024

Abstract

In astronomical observations, the estimation of distances from parallaxes is a challenging task due to the inherent measurement errors and the non-linear relationship between the parallax and the distance. This study leverages ideas from robust Bayesian inference to tackle these challenges, investigating a broad class of prior densities for estimating distances with a reduced bias and variance. Through theoretical analysis, simulation experiments, and the application to data from the *Gaia* Data Release 1 (GDR1), we demonstrate that heavy-tailed priors provide more reliable distance estimates, particularly in the presence of large fractional parallax errors. Theoretical results highlight the “curse of a single observation,” where the likelihood dominates the posterior, limiting the impact of the prior. Nevertheless, heavy-tailed priors can delay the explosion of posterior risk, offering a more robust framework for distance estimation. The findings suggest that reciprocal invariant priors, with polynomial decay in their tails, such as the Half-Cauchy and Product Half-Cauchy, are particularly well-suited for this task, providing a balance between bias reduction and variance control.

Keywords: parallax estimation, heavy-tails, credence, Bayes.

¹Department of Statistics, University of Wisconsin-Madison. sghosh39@wisc.edu

²School of Industrial Engineering, Purdue University. chatteru@purdue.edu

³Department of Statistics, Virginia Tech. jyotishka@vt.edu

*The last author was inspired to explore this problem by Professor Nick Polson and a blog-post by Professor Christian Robert ([Robert, 2016](#)), from which the title of this paper is also adapted.

1 Introduction

A parallax refers to the apparent shift in the position of an object when observed from two different vantage points. In the context of stellar astronomy, annual parallax is the most common form, which is the apparent displacement of a star observed from Earth at opposite points in its orbit around the Sun. [Ferne \(1975\)](#) pens down the rich history of studying stellar parallaxes in astronomy. With the advent of modern astronomy, technological advancements have led to highly precise measurements of parallaxes, particularly through space-based observatories like the *Hipparcos* and *Gaia* missions. Accurate distance measurements are crucial for determining the intrinsic properties of stars, such as their luminosity, mass, and size. In this endeavor, parallax measurements provide the most direct and reliable method for determining the distances to stars close to Earth. [Reid and Menten \(2020\)](#) revisits the first stellar parallaxes to estimate distances. The underlying principle involves measuring the apparent motion of a star against a distant background as the Earth orbits the Sun. By observing a star at opposite points in Earth's orbit (six months apart), astronomers can measure the angle of apparent shift in the star's position. The distance to a star (in parsecs) given by r can be calculated as the reciprocal of the parallax angle ω in arcseconds using the reciprocal relation $r = 1/\omega$.

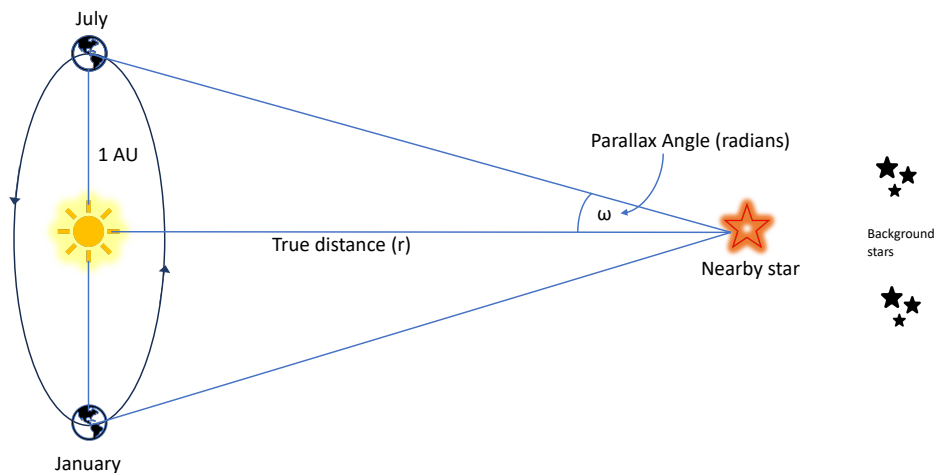


Figure 1: Trigonometric estimation of distances from stellar parallaxes

This relationship can be best understood through basic trigonometry, if we take the Earth-Sun distance (1 Astronomical Unit) as the baseline for the triangle in Figure 1, the distance to the star and the parallax angle are related as $\tan \omega = 1 \text{ AU}/r$. For small angles ω , which typically occur even for stars not too far from Earth, $\tan \omega \approx \omega$ when ω is measured in radians. The approximate relation then becomes: $r \approx 1 \text{ AU}/\omega$. When ω is measured in arcseconds, r is given in parsecs (pc), where 1 parsec corresponds to the distance at which a star would have a parallax angle of 1 arcsecond. Although, we get a simple relation between the two, inverting a parallax to give a distance is only appropriate when we have no measurement errors, which is an unrealistic assumption to make in

practical use-cases. [Bailer-Jones \(2015\)](#) argues that estimating distances from parallaxes is not trivial, especially when the fractional parallax error is large (greater than 20%). Thus, determining the distance from a parallax measurement is translated into an inference problem, which in its simplest version is estimating the distance r and its associated uncertainty σ_r , given the parallax ω and its uncertainty σ_ω .

We consider the following (simplified) model, as presented in existing literature on parallax estimation ([Bailer-Jones, 2015](#); [Astraatmadja and Bailer-Jones, 2016](#)). Denoting the observed parallax as ω , a noisy measurement corresponding to the true distance r , the likelihood is:

$$\omega \mid r, \sigma_\omega \sim \mathcal{N}\left(\frac{1}{r}, \sigma_\omega^2\right) \Rightarrow P(\omega \mid r, \sigma_\omega) = \frac{1}{\sqrt{2\pi}\sigma_\omega} \exp\left[-\frac{1}{2\sigma_\omega^2} \left(\omega - \frac{1}{r}\right)^2\right], \quad (1)$$

$$L(r \mid \omega) \propto \exp\left[-\frac{1}{2\sigma_\omega^2} \left(\frac{1}{r^2} - 2\frac{\omega}{r}\right)\right]. \quad (2)$$

It is assumed that σ_ω is known, is independent of ω , and can be estimated from another measurement model using other measured data ([de Bruijne, 2012](#)). Given the parallax ω and its uncertainty σ_ω , the statistical challenge is to derive an accurate estimate of the true distance r . Although this is rooted to one of the simplest and the most well-studied models namely, the Normal model, the problem is far from trivial! The complications in inference of the distance r arises due to the following two primary reasons: firstly, we have a *single parallax measurement*. This limitation arises due to various factors such as the limited operational lifetimes of observatories, the faintness of distant stars making repeated measurements challenging, or the substantial time and resource commitments required for multiple observations. The second challenge is induced by the inverse (nonlinear) relationship between parallax and distance: even a symmetrical error in parallax will lead to an asymmetrical error in the derived distance.

As an initial exploration, we plot the likelihood in (2) as a function of r for a fixed value of $\sigma_\omega = 1$ to exhibit the effect of observed ω on the shape and the tails of the likelihood (see Figure 2). As noted from Figure 2, for large ω values (e.g., 10, 100), the likelihood tails off quickly as r increases, indicating that very large distances become highly improbable. The peaks of the likelihood function become more distinct and sharper around $r = 1/\omega$. For smaller ω values (e.g., 0.01, 0.1), contrary to a rapid decline, the likelihood exhibits a pronounced tail extending towards larger r . This indicates that even though the most likely estimate of r is near $1/\omega$, there is a significant probability attributed to larger distances. This tail behaviour can be attributed to the fact that the transformation from parallax to distance $r = 1/\omega$ is non-linear, complicating the propagation of errors. For small parallaxes (i.e., large distances), the distribution of $1/\omega$ becomes highly skewed and long-tailed. This skewness and heavy tails in the distribution of estimated distances indicate that standard statistical methods, which often assume normality or symmetric distributions, may not perform well. Thus, it is easy to see that the naïve approach of constructing a credible region with $1/\omega \pm \sigma_\omega/\omega^2$ using the Delta method is unreliable and noisy, especially near the origin ([Bailer-Jones, 2015](#)).

It also follows from (2) that the Fisher's information for r is given by:

$$I(r) = -\mathbb{E}\left[\frac{\partial^2 \ell(r)}{\partial r^2}\right] = -\mathbb{E}\left[\frac{1}{\sigma_\omega^2} \left(\frac{2\omega}{r^3} - \frac{3}{r^4}\right)\right] = \frac{1}{\sigma_\omega^2 r^4} \quad (3)$$

The Fisher's information (3) is unbounded near $r = 0$, which in turn indicates high sensitivity of inference near the origin, i.e., small changes in the parameter around 0 result in large changes in

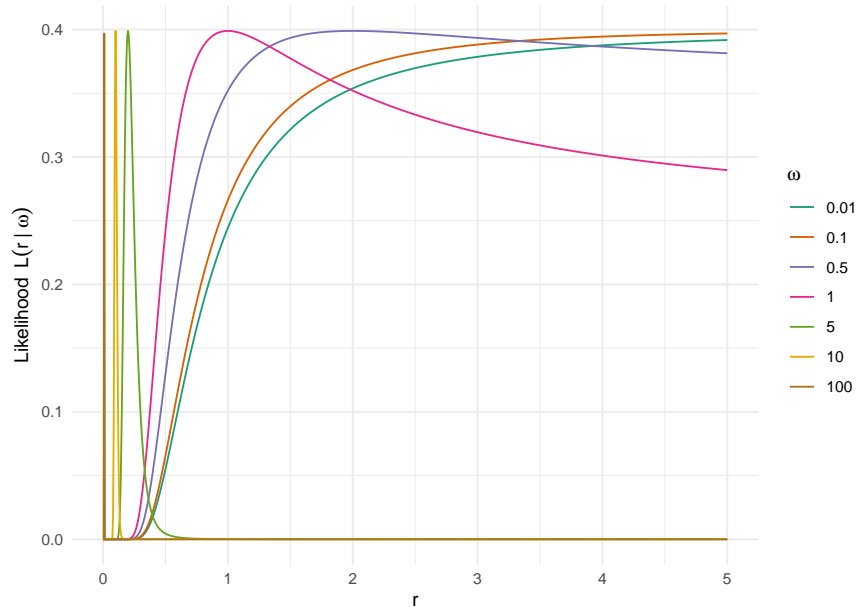


Figure 2: Plot of the likelihood as a function of r for $\sigma_\omega = 1$ to show the effect of ω on the tail-behaviour.

the likelihood. This could indicate that the model is extremely sensitive to the value of r when it is close to 0.

Estimating the reciprocals and ratios of means and regression coefficients have been investigated thoroughly in the frequentist literature (e.g. Zellner, 1978; Kuh and Meyer, 1955). For example, the Minimum Expected Loss (MELO) estimators have been proposed specifically for estimating the reciprocal means of Normal populations (Zellner and Park, 1979). They offer promising alternatives as estimators in problems where the maximum likelihood estimators do not possess finite moments and have infinite risk relative to quadratic and many other loss functions. In our setting, we can derive the MELO estimator of the distance r under the quadratic loss as $\omega/(\omega^2 + \sigma_\omega^2)$, whereas the MLE is given by $1/\omega$. Note that although the MELO estimator attempts to mitigate some of the issues with direct reciprocal estimation by incorporating σ_ω^2 in the denominator attempting to stabilize the variance, it still faces the wrath of variance explosion as ω gets close to zero.

Given the challenges with both the MLE and MELO estimators, a Bayesian approach offers a conceptual advantage by incorporating prior knowledge about the distribution of r . However, since we have a single observation, it is not favourable in terms of checking whether the prior is at all correctly specified, which can lead to biased or misleading estimates. However, there does exist a class of default priors, named Single Observation Unbiased Priors (SOUP) which can be obtained if the corresponding posterior mean of the parameter based on a single observation is an unbiased estimator of the parameter (Meng and Zaslavsky, 2002). By ensuring that the posterior distribution is unbiased with just a single observation, SOUP priors guard against the skewness induced by poorly chosen priors by aligning the posterior more closely with the actual data characteristics. Unfortunately, it has been well established that SOUP priors do not exist for non-linear transformations of Normal mean parameters (Meng and Zaslavsky, 2002; Hartigan, 1998).

From an objective Bayesian perspective, our main question is: “How do we build a suitable

prior for such a likelihood shape?” [Bailer-Jones \(2015\)](#) compared different priors and shows that the improper uniform prior or the even the prior with a sharp cut-off at some distance give very poor distance estimates (large bias and variance), and prescribed using a prior that asymptotically decays to zero at infinity, based on empirical evidences. More recently, [Bailer-Jones and others \(2021\)](#) presented a methodology for estimating distances to stars using data from *Gaia* Early Data Release 3. The study introduced geometric and photo-geometric distance estimates, utilizing a new three-parameter distance prior that replaces the simpler exponential model used in previous works. This approach enhances the precision of distance estimates across the sky by using advanced statistical models that better accommodate the complex spatial distribution of stars within our galaxy. However, it was still not robust enough to handle large fractional parallax errors. In sections 5 and 6, we demonstrate that heavy-tailed priors with polynomial tail decay rates indeed work better for this problem compared to priors with exponentially decaying tails. This aligns with the philosophy articulated in [Gelman \(2006a\)](#), which posits that “a prior can in general only be interpreted in the context of the likelihood with which it will be paired.” The suitability of heavy-tailed priors in our context is also supported by seminal papers in Bayesian robustness literature, such as [Dawid \(1973\)](#), who argued that the prior “should not wag its tail too vigorously” in order to effectively reject outliers for location families.

We turn to the notions of credence ([O’Hagan, 1990](#)) and p-credence ([Angers, 2000](#)), which helps to characterize overall “thickness” of a prior distribution’s tails beyond just the extreme ends. Our theoretical exploration leads to several key insights including the fact that, the likelihood, particularly in the case of a single observation, tends to dominate the posterior, overshadowing the influence of the prior. This phenomenon is encapsulated in our discussion detailed in Section 5 as the “curse of a single observation,” where we highlight how heavy-tailed priors, despite their robust properties, may not substantially alter the posterior relative to the likelihood.

The paper is segmented as follows. A short history of heavy-tailed priors in Bayesian literature and the ideas of regular variation and credence are described in Section 2. Existing approaches, as elucidated in [Bailer-Jones \(2015\)](#); [Astraatmadja and Bailer-Jones \(2016\)](#), are briefly reviewed and remarked upon in Section 3. Our proposed priors with rationale behind each of the candidates is in Section 4. The theoretical results involving p-credence of the posterior and comparing the growth rates of r with $1/\omega$ are provided in Section 5. We demonstrate the clear advantage of using polynomial-type decay priors over exponential-type decay priors through an elaborate simulation experiment in Section 6. The *Gaia* Data Release 1 (GDR1) dataset is analyzed in Section 7 by contrasting their naive inverse parallax estimates against our posterior distance estimates. We conclude the paper with a brief discussion in Section 8. The proofs of some of our theoretical results along with MCMC diagnostics for the simulation results and posterior predictive checks are specified in the Appendix.

2 Heavy-tailed priors: Regular Variation and Credence

Our choice of prior builds upon the long and rich history of heavy-tailed distributions in probability theory and Bayesian robustness modeling to resolve conflicts between the prior and likelihood, going back to [de Finetti \(1961\)](#); [Lindley \(1968\)](#), and [Dawid and others \(1973\)](#), and more recently [O’Hagan \(1979, 1990\)](#); [Andrade and O’Hagan \(2006, 2011\)](#); [O’Hagan and Pericchi \(2012\)](#). Various properties of these heavy-tailed priors were utilized in designing continuous shrinkage priors for

high-dimensional parameter space. Such shrinkage priors provide two simultaneous benefits: first, a spike at zero that helps squelching small, noisy parameters closer to zero and the thick tails for robustness in the tails. The latter is ensured by a result by [Barndorff-Nielsen and others \(1982\)](#) who showed that for any mixing distribution with slowly-varying tail behavior, the corresponding normal variance mixture will also have slowly varying tails. These are the so-called ‘global-local’ shrinkage priors ([Bhadra and others, 2019](#)), with the most popular method being the ‘horseshoe’ prior ([Carvalho and others, 2010](#)), so named for the induced $\text{Beta}(1/2, 1/2)$ prior on the shrinkage factors. The horseshoe prior and its many variants have been immensely popular in the Bayesian literature for the last 15 years and have attained ‘state-of-the-art’ status for high-dimensional data with low-dimensional structures (see [Bhadra and others, 2019](#)).

We provide a brief history of the heavy-tailed distributions, as it relates to our current problem. First, a random variable Z is defined to have a regularly-varying right-tail if it satisfies $P(Z > x) = x^{-\alpha}L(x)$, for $x > 0$, where $L(\cdot)$ is a slowly varying function. Recall that, a positive measurable function $L(\cdot)$ is said to be regularly varying at ∞ with index $\alpha \in \mathbb{R}$ if it is defined on some non-empty neighbourhood $[x_0, \infty)$ and $\lim_{x \rightarrow \infty} L(tx)/L(x) = t^\alpha$ for all $t > 0$. In other words, a non-negative random variable Z is regularly varying with index α if its survival function or the right distribution tail $\bar{F}_Z(\cdot)$ is regularly varying (RV, henceforth) with index $-\alpha$. One of the many interesting properties of regularly varying function is the Karamata’s theorem, which essentially states that integrals of RV functions are RV and one can take the slowly varying function out of the integral ([Mikosch, 1999](#)). A consequence of these results is the famous result by [Barndorff-Nielsen and others \(1982\)](#) concerning normal mean-variance mixtures. We state it below.

Property 1 (Theorem 6.1 of [Barndorff-Nielsen and others \(1982\)](#)). *Let $g(\cdot)$ be a normal scale mixture, with $g(x) = \int_0^\infty e^{-\frac{x^2}{2\sigma}} p(\sigma) d\sigma$, where the tail of the mixing density satisfies: $p(\sigma) \sim e^{-\psi_+ \sigma} \sigma^{\lambda-1} L(\sigma)$, ($\sigma \rightarrow \infty$). Then, we have:*

$$g(x) \sim \begin{cases} (2\pi)^{-\frac{1}{2}} 2^{\frac{1}{2}-\lambda} \Gamma(\frac{1}{2} - \lambda) |x|^{2\lambda-1} L(x^2) & \text{if } \psi_+ = 0, \\ (2\psi)^{-\frac{1}{2}\lambda} L(|x|) (|x|)^{\lambda-1} \exp(-(2\psi_+) |x|) & \text{if } \psi_+ > 0, \end{cases}$$

as $|x| \rightarrow \infty$.

This implies that the normal scale mixture distributions must have RV tails if the mixing distributions have RV tails themselves. Both the horseshoe and horseshoe+ priors are examples of normal scale mixtures with RV mixing densities, viz., Half-Cauchy and a product of Half-Cauchy’s (see Section 4) and it follows by a simple application of the above result that the priors themselves have RV tails. However, while RV tails offer a powerful tool to characterize the asymptotic behavior of distributions, they do not provide a complete picture of the ‘‘thickness’’ of the distribution’s tails across its entire domain. This is where the concept of *credence* becomes valuable.

Credence, as defined by [O’Hagan \(1990\)](#), provides a more comprehensive measure that captures not just the tail behavior but the overall thickness of the distribution.

Definition 2 ([O’Hagan \(1990\)](#)). *A density f on \mathbb{R} has a credence c if, there exist constants $0 < k \leq K < \infty$ such that for all $x \in \mathbb{R}$ we have,*

$$k \leq (1 + x^2)^{c/2} f(x) \leq K. \tag{4}$$

We write $\text{cred}(f) = c$.

A credence of $c < \infty$ ensures that for large $|x|$, $f(x)$ is of the order $|x|^{-c}$. While the idea of credence is one of its kind in a wide class of problems where we might wish to consider distributions whose tails are similar to the tails of a Student's t distributions, it encompasses only a small class of densities. In fact, the credence of the normal distribution, which is of paramount importance to us, being the likelihood, has infinite credence. Thus, no matter the choice of our prior, whether it has finite or infinite credence, the posterior will always have an infinite credence (O'Hagan, 1990). This makes it difficult to study or compare the tail properties of the prior distribution because the posterior's tail behavior is dominated by the likelihood. In that regard, Angers (2000) defined the generalized exponential power distribution (see Definition 9 in the Appendix 9) to accommodate for the logarithmic, polynomial and exponential tail behaviors in the original notion of credence by introducing p -credence.

Definition 3 (Angers (2000)). A density f on \mathbb{R} has p -credence $(\gamma, \delta, \alpha, \beta)$ if there exist constants $0 < k \leq K < \infty$ such that for all $x \in \mathbb{R}$ we have,

$$k \leq \frac{f(x)}{p(x | \gamma, \delta, \alpha, \beta)} \leq K. \quad (5)$$

Where $p(x | \gamma, \delta, \alpha, \beta)$ is a density from the Generalized Exponential Power family defined in (7). We write, $p\text{-cred}(f) = (\gamma, \delta, \alpha, \beta)$.

It is to be noted that p -credence is defined for most of the usual symmetric densities supported on \mathbb{R} (e.g. Normal, Student's- t , Laplace etc.). The introduction of p -credence allows for a unified framework to study a wide variety of tail behaviors –

- (i) Logarithmic tails when $\beta \neq 0$
- (ii) Polynomial tails when $\alpha \neq 0$
- (iii) Exponential tails when $\gamma \neq 0$

However, we are particularly interested in using the notion of p -credence to study the ‘dominance’ relation between the densities of our prior and the likelihood. The meaning of a density f ‘dominating’ another density g is outlined in the following definition.

Definition 4. Let f and g be any two densities on \mathbb{R} . We say that,

- (i) f dominates g if there exists a constant $k > 0$ such that,

$$f(x) \geq kg(x) \quad \forall x \in \mathbb{R} :$$

We write, $f \succeq g$.

- (ii) f is equivalent g if both $f \succeq g$ and $g \succeq f$. We write, $f \approx g$;
- (iii) f strictly dominates g , if $f \succeq g$ but $g \not\succeq f$.

The following proposition poses a sufficient condition to establish the dominance relation through p -credence.

Lemma 5 (Proposition 1 in [Angers \(2000\)](#)). *Let f and g be two densities on \mathbb{R} such that $p\text{-cred}(f) = (\gamma, \delta, \alpha, \beta)$ and $p\text{-cred}(g) = (\gamma', \delta', \alpha', \beta')$, then*

(i) $f \approx g$ if $\gamma = \gamma', \delta = \delta', \alpha = \alpha'$ and $\beta = \beta'$.

(ii) $f \succ g$ if:

(a) $\gamma' > \gamma$;

(b) $\gamma' = \gamma, \delta' > \delta$;

(c) $\gamma' = \gamma, \delta' = \delta, \alpha' < \alpha$;

(d) $\gamma' = \gamma, \delta' = \delta, \alpha' = \alpha, \beta' < \beta$;

The proof of this lemma is purely technical and is elaborated in [Angers \(2000\)](#). We can interpret the strict dominance ($f \succ g$) in the following manner:

(a) $\gamma' > \gamma$: The parameter γ controls the exponential tail behavior. If $\gamma' > \gamma$, the density g has a heavier (slower-decaying) tail than f . This means f decays faster at the tails than g , making f dominate g because f places less probability mass in the tails compared to g .

(b) $\gamma' = \gamma$ **and** $\delta' > \delta$: When $\gamma' = \gamma$, the densities f and g have similar exponential tail decay rates. However, δ influences the scale of this decay. If $\delta' > \delta$, g decays more slowly than f , leading to f dominating g because f again places less mass in the tail regions.

(c) $\gamma' = \gamma, \delta' = \delta$, **and** $\alpha' < \alpha$: Here, α influences the polynomial decay of the tails. If γ and δ are equal, but $\alpha' < \alpha$, then g has a thicker tail in the polynomial sense, meaning f dominates g by decaying faster polynomially.

(d) $\gamma' = \gamma, \delta' = \delta, \alpha' = \alpha$, **and** $\beta' < \beta$: Finally, if all other parameters are equal, but $\beta' < \beta$, the logarithmic decay influences the dominance relation. A lower β' means g has a slower logarithmic decay than f , making f dominate g by decaying faster logarithmically.

The conditions laid out in Lemma 5 provide clear guidelines for constructing priors that either complement or dominate the likelihood. If robustness is desired, one might choose a prior that dominates the likelihood, ensuring that the posterior is not overly influenced by potentially outlier-prone data, which in our case translates to having small values of the parallax ω .

3 Existing Approaches

Traditional frequentist approaches do not tend to work in this scenario, as correctly pointed out by [Bailer-Jones \(2015\)](#) and [Astraatmadja and Bailer-Jones \(2016\)](#). From the measurement model itself, we can infer that for $1/r$ the combined intervals $[\omega - 2\sigma_\omega, \omega]$ and $[\omega, \omega + 2\sigma_\omega]$ contain about 95.4% of the total probability of the distribution $P(\omega|r, \sigma_\omega)$. Inverting, for r , each interval $[1/\omega, 1/(\omega - 2\sigma_\omega)]$ and $[1/(\omega + 2\sigma_\omega), 1/\omega]$ tend to have the same coverage probability since the transformation $1/r \rightarrow r$ is monotonic and hence preserves the probability. Suppose, if we have a large fractional parallax error $f = \sigma_\omega/\omega = 1/2$, the upper distance interval becomes $[1/\omega, \infty)$ – which makes the

confidence interval non-informative, as some finite amount of probability in the likelihood will always correspond to an undefined distance.

The natural inclination is to resort to a Bayesian approach where we try to infer the distance in a probabilistic sense if we adopt a prior assumption about it, independent of the parallax we have observed. [Bailer-Jones \(2015\)](#) compared four different priors on r , *viz.*

1. **An improper uniform:** $\pi(r) = \mathbb{I}\{r > 0\}$, which in turn leads to an improper posterior (see Fig. 2). We would also like to note that an improper uniform is not considered non-informative in the strictest sense (see e.g. [Gelman and others, 2014](#); [Jeffreys and Swirles, 1972](#)).
2. **A proper uniform:** $r \sim \mathcal{U}(0, r_{\text{lim}})$, where r_{lim} is the maximum expected distance of a star in our galaxy, e.g. $r_{\text{lim}} = 10^3$ pc.
3. **A ‘constant volume density’ prior:** With r_{lim} having the same interpretation, the constant volume density prior is given by:

$$\pi_{cv}(r \mid \omega, \sigma_\omega) = \frac{r^2}{\sigma_\omega} \exp \left[-\frac{1}{2\sigma_\omega^2} \left(\omega - \frac{1}{r} \right)^2 \right] \mathbb{I}\{0 \leq r \leq r_{\text{lim}}\}.$$

4. **An exponentially decreasing (ED) volume density prior:** This is equivalent to a Gamma $(3, 1/L)$ prior, replaces the sharp truncation by a tapering tail, *i.e.*

$$\pi_{\text{ED}}(r \mid L) = \frac{1}{2L^3} r^2 \exp \left(-\frac{r}{L} \right).$$

Beyond this point, we will use the terms Gamma and ED priors interchangeably throughout the manuscript. The superior performance of the ED prior in reducing bias and variance in estimated distances, particularly when using the posterior mode has been highlighted in previous literature ([Bailer-Jones, 2015](#); [Astraatmadja and Bailer-Jones, 2016](#)). This advantage holds notably under conditions of non-positive parallaxes and inevitably, large fractional parallax errors: $f_{\text{true}} = \sigma_\omega r_{\text{true}} \leq 0.4$, where r_{true} is the true distance taken into the simulation setting. Simulation results demonstrate a stark contrast in performance among different priors: the standard deviation of the posterior mode for the improper uniform prior sharply increases as f_{true} surpasses 0.2. Although the proper uniform prior shows slight improvement, maintaining stability until f_{true} reaches 0.25, it still under-performs compared to the constant volume density prior, which robustly controls the standard deviation of the posterior mode up to a f_{true} of 0.35.

4 Proposed Methodology

4.1 Heavy-tailed priors for Parallax Estimation

[Bailer-Jones \(2015\)](#)’s suggestions have been instrumental in the choice of informative priors for solving the problem of exploding standard deviations of the posterior estimators. He does not recommend the use of a prior with a sharp cutoff (for instance, the proper uniform prior), because it introduces significant biases for low-accuracy measurements at all distances. He endorses the idea of using a prior which converges asymptotically to zero as the distance becomes large enough. We back that idea by proposing the following heavy-tailed candidate priors:

- (i) **Reciprocal-Gaussian Prior (RG⁺):** We consider the truncated Reciprocal Gaussian prior $RG^+(0, \sigma^2)$

$$\pi(r) = \sqrt{\frac{2}{\pi}} \frac{1}{\sigma r^2} \exp\left(-\frac{1}{2\sigma^2 r^2}\right), \quad r > 0.$$

It serves as a conjugate prior to within the measurement model used. This can be observed easily while computing the posterior as follows:

$$\begin{aligned} \pi(r|\omega) &\propto \exp\left[-\frac{1}{2\sigma_\omega^2} \left\{\frac{1}{r^2} - \frac{2\omega}{r}\right\}\right] \frac{1}{r^2} \exp\left(-\frac{1}{2\sigma^2 r^2}\right) \\ &\propto \frac{1}{r^2} \exp\left[-\frac{1}{\tau_\omega^2} \left(\frac{1}{r} - \frac{\tau_\omega^2 \omega}{\sigma_\omega^2}\right)\right]. \end{aligned}$$

Where $\frac{1}{\tau_\omega^2} := \frac{1}{\sigma_\omega^2} + \frac{1}{\sigma^2}$. Implying that,

$$r|\omega, \sigma_\omega \sim RG^+\left(\frac{\tau_\omega^2 \omega}{\sigma_\omega^2}, \tau_\omega^2\right).$$

- (ii) **Inverse-Gamma prior:** Considering a small shape parameter $\alpha > 1$, it features a *heavier tail* compared to the ED prior, making it suitable for applications requiring robust handling of smaller parallax measurements. The Inverse-Gamma (ϵ, ϵ) originally proposed by [Browne and Draper \(2006\)](#), is a pretty commonly used “diffuse” prior in the literature, for small values of ϵ — sometimes a default prior in Bayesian modeling, particularly when dealing with variance components in hierarchical or mixed-effect models.
- (iii) **Half-Cauchy prior:** The Jeffrey’s Prior, based on the square root of Fisher’s Information, leads to $\pi(r) \propto \frac{1}{r^2}$ (follows from Equation 3), which has a similar tail behavior to the standard Half-Cauchy $C^+(0,1)$. Traditional Bayesian models often use an Inverse-Gamma prior for variance components. However, the Inverse-Gamma prior may induce strong shrinkage, especially when the data is limited ([Gelman, 2006b](#)). The Half-Cauchy prior, in contrast, is less informative and has been shown to perform better in many hierarchical settings, particularly when the number of groups is small. It avoids the problems associated with overly tight priors, which can lead to underestimating variability ([Polson and Scott, 2012](#)).

Remark: With $r \sim C^+(0, 1)$ one can see that for $x > 0$,

$$\begin{aligned} \mathbb{P}(r > x|\omega) &= c(\omega) \int_x^\infty \frac{1}{1+r^2} \exp\left(-\frac{1}{2\sigma_\omega^2} \left(\frac{1}{r^2} - \frac{2\omega}{r}\right)\right) \\ &\leq c(\omega) \int_x^\infty \frac{1}{r^2} \exp\left(-\frac{1}{2\sigma_\omega^2} \left(\frac{1}{r^2} - \frac{2\omega}{r}\right)\right) \\ &= c(\omega) \exp\left(-\frac{\omega^2}{2\sigma_\omega^2}\right) \mathbb{P}(RG^+ \geq x). \end{aligned} \tag{6}$$

Thus, for small values of ω , the tail behavior of the Half-Cauchy distribution increasingly resembles that of the Reciprocal Gaussian distribution.

- (iv) **Weibull Prior:** The Weibull prior with scale parameter 1 is heavy-tailed when $\alpha < 1$, exhibiting sub-exponential behavior which is useful for modeling tail risks. [Ibrahim and others \(2005\)](#) provides an in-depth treatment of extreme-value distributions, including Weibull priors for modeling survival times and hazard functions.
- (v) **Product Half-Cauchy Prior:** We propose the Product Half-Cauchy prior, typically from the standpoint of further slowing down the rate of tail decay for the Half-Cauchy prior. The product of two Half-Cauchy random variables has the following density:

$$\pi(r) = \frac{2 \log r}{r^2 - 1}, \quad r > 0$$

The tail behavior is given by $2 \log r / r^2$ as $r \rightarrow \infty$, where the presence of the $\log r$ term in the numerator actually causes the tail to be thicker than the Half-Cauchy distribution. The product of two Half-Cauchy distributions (say, τ and λ for instance) is often used as a prior for variance components in a hierarchical model. This formulation is conceptually similar to the Horseshoe prior ([Carvalho and others, 2010](#)), because it effectively shrinks small values of r towards zero while allowing large values of r to remain large due to the heavy tails of the Half-Cauchy distributions. However, it differs from the Horseshoe prior in the sense that there is no separate global and local shrinkage parameter in this single observation scenario. We note here that the prior distribution for the local shrinkage parameter in horseshoe+ prior ([Bhadra and others, 2015](#)) has a Product Half-Cauchy distribution.

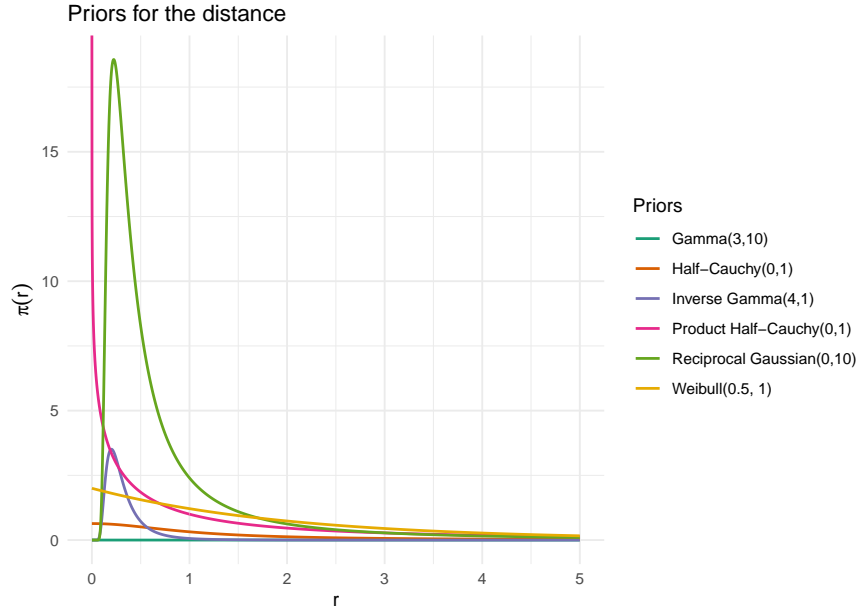


Figure 3: Tail behavior of the candidate priors

These candidate priors can be sorted in terms of their tail-heaviness according to their p-credence criteria discussed in Lemma 5 (see Table 1). Their tails can also be visualized through their density functions plotted in Figure 3. The lightest tail is exhibited by the Gamma(3, 10) prior, whereas the heaviest tail belongs to the Product Half-Cauchy(0, 1) prior.

Table 1: Sorting the priors according to tail-heaviness (Light-Heavy) (top to bottom).

Prior	Tail Decay Rate	p-credence
Gamma(n, θ)	$e^{-\theta r}$	$(1, \theta, 1 - n, 0)$
Weibull($c, 1$)	e^{-r^c}	$(c, 1, 1 - c, 0)$
Inverse-Gamma($\alpha, 1$)	$r^{-(\alpha+1)}$	$(0, 0, \alpha + 1, 0)$
Reciprocal-Gaussian($0, \sigma^2$)	r^{-2}	$(0, 0, 2, 0)$
Half-Cauchy($0, 1$)	r^{-2}	$(0, 0, 2, 0)$
Product Half-Cauchy($0, 1$)	$\frac{\log(r^2)}{r^2}$	$(0, 0, 2, -1)$

5 Theoretical Results

In our endeavour to get robust Bayesian inference, limiting the influence of conflicting information (in our case, too small values of ω), the use of heavy-tailed distributions is a valuable tool. It is natural to therefore characterize the tail behaviour of the posterior through the notion of credence and p-credence in a bid to determine the dominance of the prior or the likelihood. The prior class which greatly simplifies our inverse-mean modeling problem is the class of *reciprocal invariant* priors. Reciprocal random variables X , where $X \geq 0$ by definition, satisfy the strong invariant property $X \stackrel{d}{=} X^{-1}$. They have been characterized by the following two equivalent conditions (Hürlimann, 2011):

- (1) The functional equation

$$f(x) = \frac{1}{x^2} f\left(\frac{1}{x}\right), \quad x > 0.$$

is satisfied for f (density of X).

- (2) The transformed random variable $Y = \psi(X)$ is a symmetric random variable with respect to the origin, where $\psi : (0, \infty) \rightarrow \mathbb{R}$ is a monotone differentiable function with the property $\psi(x) = -\psi(x^{-1})$, $x > 0$.

Note that both the Half-Cauchy and the Product Half-Cauchy priors fall under the category of reciprocal invariant. The simplification of the modeling problem is subject to the following observation that for Bayesian inference involving the distance parameter r , we look into the posterior

$$\pi(r|\omega) \propto \pi(r) \exp\left(-\frac{1}{2\sigma_\omega^2} \left(\omega - \frac{1}{r}\right)^2\right).$$

Under reciprocal invariance of $\pi(r)$, if we transform $r \mapsto t := 1/r$, the posterior density looks like

$$\pi(t|\omega) \propto \pi(t) \exp\left(-\frac{1}{2\sigma_\omega^2} (\omega - t)^2\right).$$

which boils down to a Bayesian inference problem involving the location parameter t . Of course, this problem is well studied in the literature in the context of developing robust Bayesian procedures

for guarding against sample outliers and prior mis-specifications. The following results help us understand the asymptotic behavior of the posterior density for the location parameter t – the term “asymptotic” being used not in the frequentist sense, where the sample size goes to infinity, rather in the sense of having conflicting values, that is, $\omega \rightarrow 0$.

5.1 Tail Behavior of the Posterior

We restrict ourselves to the class of reciprocal invariant priors. The following result enlightens us about the tail decay rate of the posterior, considering the influence of heavy-tailed priors, courtesy [Angers \(2000\)](#).

Theorem 6. If $\text{p-cred}(L(\omega|t)) = (\gamma', \delta', \alpha', \beta')$ and the $\text{p-cred}(\pi(t)) = (0, \delta, \alpha, \beta)$, where we impose $\pi(\cdot)$ to be reciprocal invariant, then

$$\text{p-cred}(\pi(t|\omega)) = (\gamma', \delta', \alpha + \alpha', \beta + \beta')$$

when $\gamma' > 0$.

Recalling Lemma 5, we are actually interested in priors whose tail decay is slower than exponential, and thus emphasize on $\gamma = 0$ for the prior $\pi(\cdot)$. Of course, this result can be extended to any $\gamma > 0$, as already discussed in [Angers \(2000\)](#). Note that in our scenario, since we have a Normal likelihood, then $\pi \succ L$ for a sufficiently heavy-tailed prior $\pi(\cdot)$ as $\gamma' > 0$ (in fact, $\gamma' = 2$ to be exact). Theorem 6 suggests that even under the influence of a heavy-tailed prior, the posterior tail behavior is dominated by the information source with higher credence or the first p-credence coefficient γ' that is, the Normal likelihood. In fact, we can go a step further by harping on the corollary provided in [O'Hagan \(1990\)](#).

Corollary 7 (Curse of a Single Observation). The posterior probabilities for any fixed t (or, r) are bounded by positive multiples of the likelihood. Specifically, for any given $d > 0$ and $\epsilon > 0$ such that $\forall \omega < A$ and $\forall t \leq d$,

$$\frac{k'}{K^*}(1 - \epsilon) \leq \pi(t|\omega) \{L(\omega|t)\}^{-1} \leq \frac{K'}{k^*}(1 + \epsilon)$$

with appropriate positive constants k', K', k^* , and K^* .

In practical terms, this means that in situations where we have a single observation (even limited observations), the prior – no matter how heavy-tailed, will not significantly alter the posterior distribution's behavior relative to the likelihood. The likelihood “dominates” the posterior, rendering the prior's tail less impactful. We name this the “*curse of a single observation*”!

Another manifestation of this curse is observed through the following proposition, which indicates that even if the prior decays slowly enough for large r , the posterior cannot put enough mass beyond $1/\omega$, or in fact, any function $c(\omega)$ which diverges as $\omega \rightarrow 0$.

Proposition 8. Under reciprocally invariant priors with finite tail credences, for all functions $c : \mathbb{R}^+ \mapsto \mathbb{R}^+$ such that $c(x) \rightarrow \infty$ as $x \rightarrow 0$,

$$\lim_{\omega \rightarrow 0} \mathbb{P}(r > c(\omega)|\omega) = 0$$

The proofs of Theorem 6 and Proposition 8 are detailed in the Appendix 9.1.

Note: The proposition highlights that the posterior distribution cannot “keep up” with the growth rate of $c(\omega)$ as ω becomes small enough. In other words, r cannot cope with the rapid growth of $c(\omega)$ in the posterior distribution.

5.2 Posterior Risk and Prior Choices

We now broaden our scope from the class of reciprocal invariant priors to consider the larger class of non-degenerate priors. From a decision theoretic point of view, it might be of interest to study the posterior risk under common loss functions (e.g. Squared Error Loss, Absolute Error Loss etc.). Of particular importance is the quantity $\mathbb{E}[(r - r_0)^2|\omega]$ denoted by the integral $I(r_0, A)$ below, which measures the discrepancy $\delta > 0$ of the posterior distribution’s possible values of r from the true distance r_0 .

$$I(r_0, A) = \int_0^\infty \delta(r, r_0) \pi(r) \exp\left(-\frac{A}{r^2} + \frac{2\omega A}{r}\right) dr.$$

where $A = 1/2\sigma_\omega^2$

If we take δ to be the Squared Error Loss function $(r - r_0)^2$, [Bailer-Jones \(2015\)](#) have identified that $I(r_0, A)$ explodes as $r_0 \rightarrow \infty$ (that is, with increasing fractional parallax errors). This can be verified easily through the following inequalities, by fixing $A = \omega = 1$ for instance, with $r_0 \geq 2$,

$$I(r_0, 1) \geq \int_1^{r_0^2} \frac{r_0^2}{4} \pi(r) \exp\left(-\frac{1}{r^2} + \frac{2}{r}\right) dr \geq \frac{\exp\left(-\frac{1}{4}\right)}{4} \left(\int_1^{r_0^2} \pi(r) dr\right) r_0^2.$$

The rightmost term diverges to ∞ with increasing r_0 , provided that our prior is non-degenerate on $\{r > 0\}$.

No prevention, only delay! – This unbounded growth occurs regardless of the choice of prior. But, *the use of a heavy-tailed prior can “delay” the explosion of the posterior risk because it allows the posterior distribution to accommodate larger values of r more readily.* Specifically, for larger r_0 , a heavy-tailed prior places more weight on values of r that are far from the mode of the distribution. This increased spread can partially counteract the quadratic growth of the squared error loss, slowing down the rate at which $I(r_0, A)$ increases.

The natural follow-up question to ask here is, “how heavy is sufficiently heavy?” In that regard, [Desgagné and Angers \(2007\)](#) has quantified the thickness and regularity for the prior tails needed for robust location parameter inference, through three regularity conditions:

(C1) For any $\epsilon, h > 0$, there exists a constant $A_1(\epsilon, h) > 0$, such that $z > A_1(\epsilon, h)$ and $|\theta| \leq h$
 $\implies 1 - \epsilon \leq \pi(z + \theta)\pi(z)^{-1} \leq 1 + \epsilon.$

(C2) There exists a constant $M_2 > 1$ and a proper density g such that for all $z > A_2$,

$$\frac{\pi^2\left(\frac{z}{2}\right)}{\pi(z)g\left(\frac{z}{2}\right)} \leq M_2.$$

(C3)

$$\frac{d^2}{dz^2} \log \pi^*(z) \geq \frac{d^2}{dz^2} \log g(z) \geq 0,$$

where, π^* can be the density π or a density with the same tail behavior.

Remarks: The condition (C1) implies that a location transformation has no impact on the right tail of the prior density $\pi(z)$ as $z \rightarrow \infty$. For instance, if $\pi(z)$ is the density of a Half-Cauchy distribution, $\lim_{z \rightarrow \infty} \pi(z + \theta)\pi(z)^{-1} = 1$. For conditions (C2) and (C3), we can take g to be a double Pareto density as professed by [Angers \(2000\)](#). Condition (C3) ensures that the logarithm of the densities π^* , and g have convex right tails, with the log-convexity of π^* being more pronounced than that of g . It is worthwhile to note that among our list of candidate priors, these regularity conditions are satisfied by the Inverse Gamma, the Reciprocal Gaussian, the Half Cauchy, and the Product Half Cauchy priors.

6 Simulation Experiments

We define a simulation setup for assessing the performance of our candidate priors discussed in Section 4 to estimate distances from the parallax measurements. To be specific, we compare the priors Gamma (3, 10), Inverse-Gamma (4, 1), Reciprocal-Gaussian (0, 10), Weibull (0.5, 1), Half-Cauchy (0, 1), and Product Half-Cauchy (0, 1). We generate a sequence of ω 's of length $J = 500$, uniformly spaced between 0 and 8. The true value of the distance r is taken to be $\frac{1}{\omega}$ for each instance. We fix $\sigma_\omega = 0.045 \simeq 1/\sqrt{500}$, based on the suggestions of [Bailer-Jones \(2015\)](#). For practical purposes, it is generally advisable to take σ_ω depending primarily on the number of photons (N) received by the telescope from the star, or rather, its brightness. However, it has been observed that the choice of the noise parameter σ_ω plays a crucial role in determining the robustness and reliability of the model fit. By choosing a low value for σ_ω , specifically 0.045, our intent is to minimize the impact of observational noise on the model's performance – allowing for a clearer evaluation of the priors' effectiveness in estimating distances without the confounding effects of large measurement errors.

Then, we fit the hierarchical model:

$$\omega \sim \mathcal{N}\left(\frac{1}{r}, \sigma_\omega^2\right), \quad r \sim \pi(r).$$

To implement this, we use the Hamiltonian Monte Carlo algorithm, specifically the NUTS (No-U-Turn Sampler) variant, to draw samples from the posterior distribution ([Hoffman and Gelman \(2011\)](#)) using R-stan ([Carpenter and others, 2017](#)). We consider 5000 MCMC sampling iterations with 2000 warm-up iterations for a single chain. We consider the posterior median estimates \hat{r} of the true distances r for all the candidate priors. We refrain from using posterior mean estimates due to the fact that their behavior becomes erratic and unreliable when the underlying distribution lacks a theoretical mean – for instance, Reciprocal-Gaussian, Half-Cauchy, and Product Half-Cauchy fall under that category.

Our goal in this experiment is to measure the squared error $(\hat{r} - r)^2$ as a function of the true value of the fractional parallax error (f), which is defined as $\sigma_\omega \cdot r$, a measure of the relative error in the parallax estimate (see Figure 4). Note that we take the sequence of observed parallaxes (ω)'s

in such a way that f can vary widely from 0.005 to 1. Of course, we are interested in studying the behavior of the discrepancy between \hat{r} and r , when the fractional parallax error increases (or equivalently, large values of r). A few remarks are in order, based on the results observed in Figure

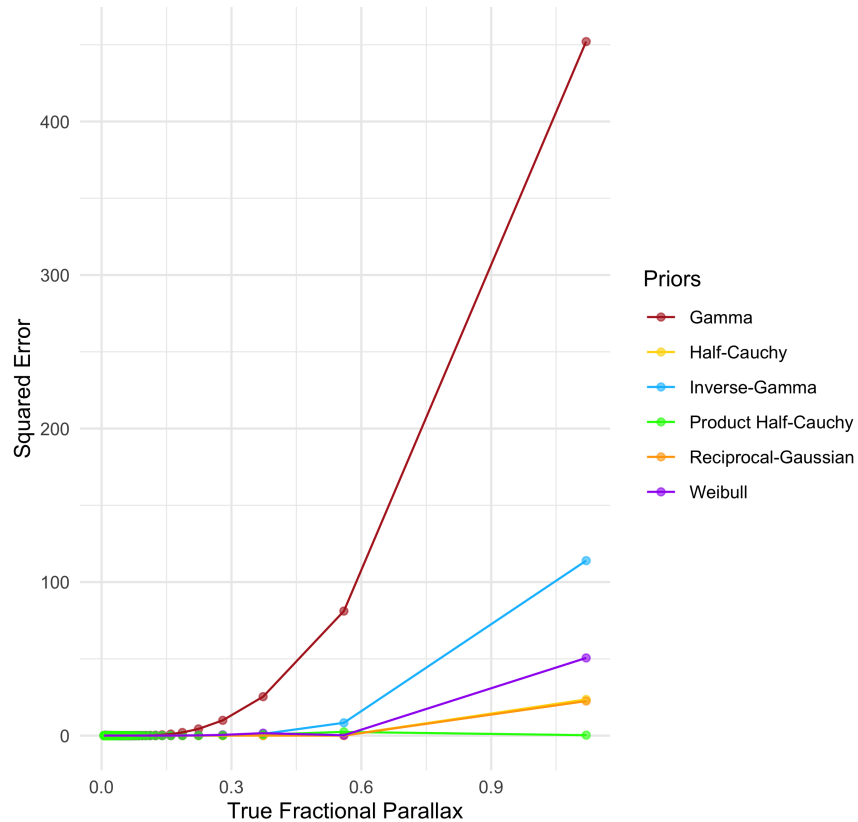


Figure 4: Plot indicating how the squared error varies with the true distance across all the candidate priors, for $\sigma_\omega = 0.045$

4:

- (1) Clearly, the Product Half-Cauchy prior demonstrates the lowest increase in squared error, maintaining close to a flat error rate as the true distance increases. With the heaviest tails among the others (see Table 1), the Product Half-Cauchy prior is the most robust in handling larger values of f . This results in the smallest increase in squared errors as r increases, which aligns with its ability to accommodate extreme values effectively without significant loss in estimation accuracy.
- (2) The Reciprocal-Gaussian and the Half-Cauchy priors show pretty similar increase in terms of squared error, which can be explained by their similarity in posterior tail probabilities, as discussed earlier in Section 4.
- (3) The explosion in squared error noted for the Gamma prior as f surpasses 0.4 is consistent with [Bailer-Jones \(2015\)](#)'s observations for the "Exponential Decay" prior.

It's important to note that the robustness of the Product Half-Cauchy, Half-Cauchy and the Reciprocal-Gaussian priors extends to large fractional parallax error thresholds (the parallax error being larger than 0.8). However, such extreme error thresholds are generally not encountered in

practice due to the high precision of modern instruments. This robustness is more of a theoretical advantage, ensuring stability and reliability of the estimation process even under conditions of unusually high measurement errors.

7 Real Data Results

We utilize an elaborate astrometric dataset extracted from the *Gaia* Data Release 1 (GDR1), which encompasses positional, parallactic, and proper motion measurements for approximately 2 million of the brightest stars. These stars are included in both the *Hipparcos* and *Tycho-2* catalogues, providing a rich source of data for precise astronomical studies. For GDR1, a complex mathematical model known as the Global Astrometric Solution (Spoto, F. and others (2017)) was used to combine the *Gaia* observations with the earlier *Hipparcos* and *Tycho-2* data. This method ensures consistency across different datasets and helps in minimizing systematic errors. Moreover, *Gaia*'s observations over multiple years (and *Hipparcos* before it) provide a long baseline for measuring parallax shifts. A longer time baseline enhances the precision of parallax measurements, as the small apparent movements of stars due to Earth's orbit around the Sun can be more accurately detected.

Our analysis focuses on computing the posterior distances for a selected sample of 100 stars. By comparing the medians of the posterior distributions derived from these priors to the naive inverse parallax estimates provided in the GDR1 database, we aim to assess the accuracy and reliability of the proposed hierarchical models. It is to be noted that the parallaxes are in mas (milli-arcseconds), and angles are in degrees in the original database. We convert the parallaxes to arcseconds so that distances come out as pc (parsecs). To make the scale of our priors consistent with the magnitude of the data and for fair comparison across the priors, we choose the common scale parameter $L = 1000$.

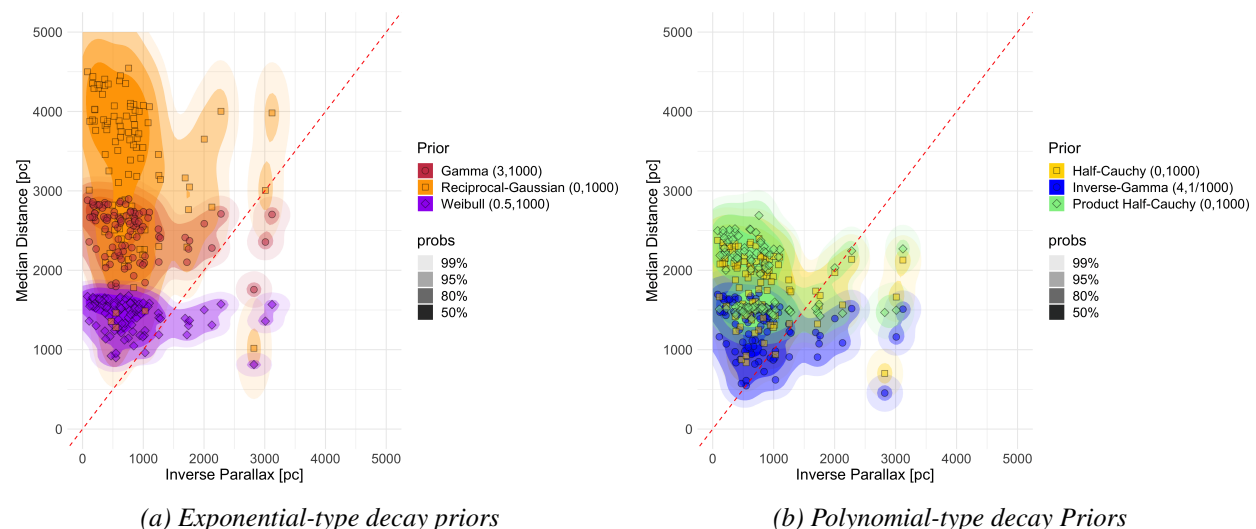


Figure 5: Plotting the posterior estimates against the naive GDR1 Inverse Parallax estimates.

The plot in Figure 5a contrasts the posterior median estimates against the tabulated GDR1 naive inverse parallax estimates for priors whose tail decay rates are exponential (see Table 1). Similarly, Figure 5b enlists and compares all the priors with heavier tails, their tail decay rates

being polynomial. The degree to which points cluster around the diagonal line (red dotted line in each figure) indicates how closely the Bayesian estimates align with the inverse parallax estimates. A tight clustering around the diagonal suggests strong agreement, while a broad scatter indicates discrepancies between the two methods.

Key Observations (Exponential-type decay Priors):

- (1) The Gamma and Reciprocal-Gaussian priors have their densest regions overlapping the naive estimates more closely, while the Weibull prior shows a broader spread with a significant chunk of its 50% confidence region lying below the identity line. This indicates that the Weibull prior might be more skeptical of the larger distance estimates provided by the naive method.
- (2) The Reciprocal-Gaussian prior has the broadest spread amongst the three light-tailed priors, suggesting that it might be allowing for more variability in the posterior estimates, especially at higher distances.

Key Observations (Polynomial-type decay Priors):

- (1) The Half-Cauchy prior tends to shrink the distance estimates compared to the naive method, especially for stars with larger parallax (shorter distances), whereas the contours for the Inverse-Gamma prior suggest that it allows for a broader range of possible distances, especially at lower values.
- (2) The Product Half-Cauchy prior appears to be more conservative, keeping estimates closer to the identity line but still showing a tendency to shrink distances compared to the naive method.

All the candidate priors produce posterior median estimates that do not perfectly align with the naive inverse parallax estimates. This misalignment is expected, as the Bayesian models incorporate additional prior information and are not solely dependent on the parallax data – which naturally introduce biases, especially in cases of large parallax errors or when the parallax is small. Polynomial-tailed priors are usually more appropriate when dealing with such scenarios, offering a more cautious approach, which can be beneficial in ensuring that the posterior estimates are not unduly influenced by extreme values.

8 Discussion

In this study, we explored the challenge of estimating stellar distances from parallax measurements, focusing on the impact of various prior distributions on Bayesian inference in this context. The reciprocal (non-linear) relationship between parallax and distance, compounded by the presence of measurement errors, complicates the task of deriving accurate distance estimates. We evaluated a range of heavy-tailed priors, possessing both exponential-type and polynomial-type decay rates. Priors with heavier tails, such as the Product Half-Cauchy and Half-Cauchy distributions, demonstrated superior robustness in handling large fractional parallax errors, maintaining lower squared errors and providing more reliable distance estimates compared to their exponential counterparts. The analysis of real data from the *Gaia* Data Release 1 (GDR1) further reinforced these findings. Posterior distance estimates derived using heavy-tailed priors were generally more conservative and exhibited a better fit to the underlying data, as evidenced by posterior predictive checks (see

Appendix 9.3).

From a theoretical standpoint, the use of reciprocal invariant priors, such as the Half-Cauchy and Product Half-Cauchy, also proved beneficial by simplifying the problem through the transformation to a location parameter. We show that while heavy-tailed priors can delay the explosion of posterior risk, the posterior is still largely dominated by the likelihood due to the “curse of a single observation.” Given these considerations, we recommend that *practitioners use the class of reciprocal invariant priors—such as the Half-Cauchy and Product Half-Cauchy distributions—that satisfy the three regularity conditions ((C1)–(C3)) for tail thickness given in Section 5*. These criteria provide a robust framework for inference in the presence of significant uncertainty in the parallax measurements, ensuring that the posterior distribution remains well-behaved even under the challenging conditions of observing small parallaxes.

However, it is important to note that the class of reciprocal invariant priors satisfying these three regularity conditions is not exhaustive for obtaining good inference for r . One can construct a prior, such as the product of a Half-Cauchy and a Reciprocal-Gaussian distribution, which is not reciprocal invariant but still exhibits similar tail behavior to the Product Half-Cauchy prior. We term that prior as “Reciprocal-Horseshoe” since, the density of its reciprocal random variable resembles the density of a Horseshoe prior. This suggests that other compositions of priors, beyond the reciprocal invariant class, might also yield robust estimates. Whether there exists a broader class of such composite priors that could be systematically explored for this and similar problems is an intriguing question and remains a topic for future research.

Another important question that arises from this study is the choice of loss function for evaluating different estimators. Given the information asymmetry and the non-linear nature of the problem, a pertinent question that still needs to be settled is if the squared error loss a reasonable choice for this problem. Exploring alternative loss functions that might better reflect the underlying complexities of the distance estimation problem could lead to more accurate and meaningful evaluations of estimator performance. We hope to pursue this problem in a future study.

In conclusion, the findings from this study provide a clear direction on the efficacy of heavy-tailed priors for robust Bayesian inference on estimating astronomical distances, contributing valuable insights that can aid in the precise mapping of the cosmos.

Acknowledgments

The authors would like to thank Sameer Deshpande and Jessi Cisewski-Kehe for their helpful comments and encouragement.

9 Appendix

9.1 Theoretical Proofs

We present the proofs of Theorem 6 and Proposition 8 in this section.

Before stating the proof, we define the following rich class of densities introduced in [Angers \(2000\)](#).

Definition 9. (*Generalized Exponential Power Family*)

The class of distributions with density:

$$p(z|\gamma, \delta, \alpha, \beta) \propto \max(|z|, z_0)^\alpha \log^\beta(\max(|z|, z_0)) \exp(-\delta \max(|z|, z_0)^\gamma) \quad (7)$$

satisfying:

- (1) $z_0 > 1$, if $\beta \neq 0$; or $z_0 > 0$, if $\alpha < 0, \beta = 0$
- (2) $\alpha + \frac{\beta}{\log(z_0)} \leq \delta \gamma z_0^\gamma$
- (3) $\alpha \leq -1$, if $\gamma = 0$
- (4) $\beta < -1$, if $\gamma = 0$ and $\alpha = -1$

Proof. (Proof of Theorem 6) Without loss of generality assume that $z_0 > 0$ in (7). The key observation here is the following, courtesy Lemma 1 in Angers (2000),

If $c \neq 0, d \in \mathbb{R}$, then $\forall z \in \mathbb{R}$, there exists constants $0 < a \leq A < \infty$ such that

$$a \leq \frac{\max(|z|, z_0)}{\max(|cz + d|, z_0)} \leq A \quad (8)$$

Recall that the $\text{p-cred}(L(\omega|t)) = (\gamma', \delta', \alpha', \beta')$ and the $\text{p-cred}(\pi(t)) = (0, \delta, \alpha, \beta)$. Define $m(\omega)$ to be the marginal distribution of ω . Using the above result (8) and the definition of p-credence , it's straightforward to observe that for constants $A, K, K' > 0$:

$$\begin{aligned} \pi(t|\omega) &= \frac{L(\omega|t)\pi(t)}{m(\omega)} \\ &\leq \frac{KK'}{m(\omega)} \max(|t|, z_0)^\alpha \max(|t - \omega|, z_0)^{\alpha'} \log^\beta[\max(|t|, z_0)] \\ &\quad \log^{\beta'}[\max(|t - \omega|, z_0)] \exp\left\{-[\delta' \max(|t - \omega|, z_0)^{\gamma'}]\right\} \\ &\leq \frac{AKK'}{m(\omega)} \max(|t - \omega|, z_0)^{\alpha+\alpha'} \log^{\beta+\beta'}[\max(|t - \omega|, z_0)] \\ &\quad \exp\left[-\delta' \max(|t - \omega|, z_0)^{\gamma'}\right] \end{aligned} \quad (9)$$

Similarly, we can have a similar lower bound using (8), where there exists constants $a, k, k' > 0$ such that:

$$\begin{aligned} \pi(t|\omega) &\geq \frac{akk'}{m(\omega)} \max(|t - \omega|, z_0)^{\alpha+\alpha'} \log^{\beta+\beta'}[\max(|t - \omega|, z_0)] \\ &\quad \exp\left[-\left\{\delta' \max(|t - \omega|, z_0)^{\gamma'}\right\}\right] \end{aligned} \quad (10)$$

Combining the bounds (10) and (9), we have that

$$\pi(t|\omega) \approx p(t - \omega|\gamma', \delta', \alpha + \alpha', \beta + \beta')$$

and the result follows. \square

For proving the next result, let us denote the likelihood $L(\omega|t)$ as $g(r - \omega^{-1})$ by mere re-parametrization. Define the $\text{credence}(\pi) = c$, and the $\text{credence}(g) = c'$. From our model, it is clear that $c' > c$.

Proof. (**Proof of Proposition 8**) Following the lines of [O'Hagan \(1990\)](#), we first prove that for all $a > 0$,

$$\mathbb{P}(r > a\omega^{-1}|\omega) \rightarrow 0, \text{ as } \omega \rightarrow 0$$

Also, from Theorem 2 of [O'Hagan \(1990\)](#), we know that the credence of the marginal distribution $m(\omega^{-1})$ is given by $\min(c, c') = c$. Thus, we can see that:

$$\begin{aligned} \mathbb{P}(r > a\omega^{-1}|\omega) &= (m(\omega^{-1}))^{-1} \int_{a\omega^{-1}}^{\infty} \pi(r)g(r - \omega^{-1})dr \\ &\leq K(1 + \omega^{-2})^{\frac{c}{2}} \int_0^{\infty} \pi(m + (a + 1)\omega^{-1})g(m + a\omega^{-1})dm \\ &\leq \frac{K}{k'}(1 + \omega^{-2})^{\frac{c}{2}}(1 + a^2\omega^{-2})^{-\frac{c'}{2}} \int_0^{\infty} \pi(m + (a + 1)\omega^{-1})dm \\ &< \frac{K}{k'}(1 + \omega^{-2})^{\frac{c}{2}} \cdot (1 + a^2\omega^{-2})^{-\frac{c'}{2}} \rightarrow 0, \text{ as } \omega \rightarrow 0 \end{aligned}$$

where the transformation in the second step is given by $\omega^{-1} - r \mapsto m + a\omega^{-1}$. Now, if $c(\omega) \rightarrow \infty$ faster than $a\omega^{-1}$, then compute the following:

$$\begin{aligned} \mathbb{P}(c(\omega) < r < a\omega^{-1}|\omega) &= m(\omega^{-1})^{-1} \int_{c(\omega)}^{a\omega^{-1}} \pi(r)g(r - \omega^{-1})dr \\ &\leq \frac{(1 + \omega^{-2})^{\frac{c}{2}}}{k^*} \int_{c(\omega)}^{a\omega^{-1}} \pi(r)g(r - \omega^{-1})dr \\ &\leq \frac{K'}{k^*}(1 + \omega^{-2})^{\frac{c}{2}}(1 + c(\omega)^2)^{-\frac{c}{2}} \int_{c(\omega)}^{a\omega^{-1}} g(r - \omega^{-1})dr \end{aligned}$$

where k', K, K', k^* are the constant multipliers associated with the credences of g, m , and π respectively.

Since, $c(\omega)$ grows faster than ω^{-1} as $\omega \rightarrow 0$, we can argue that for small enough ω , $c(\omega) > A\omega^{-1}$, where $A > 0$ is a constant. Thus, the limiting value of the quantity $\lim_{\omega \rightarrow 0} \left[\frac{1 + \omega^{-2}}{1 + c(\omega)^2} \right]^c < \lim_{\omega \rightarrow 0} \left[\frac{1 + \omega^{-2}}{1 + A^2\omega^{-2}} \right]^c \rightarrow A^{-2c} < \infty$.

The proof is completed by observing that the integral $\int_{c(\omega)}^{a\omega^{-1}} g(r - \omega^{-1}) \rightarrow 0$ as $\omega \rightarrow 0$. \square

9.2 Convergence Diagnostics

To assess the convergence and efficiency of the MCMC sampling process for different prior distributions in our simulation setting (Section 6), we calculated the mean R-hat ([Gelman and Rubin \(1992\)](#)) and mean Effective Sample Size (ESS) ([Geyer \(1992\)](#)) for each prior. The R-hat statistic measures convergence, with values close to 1.0 indicating good mixing of the chains. The ESS quantifies the effective number of independent samples, with higher values suggesting more efficient sampling.

Table 2 summarizes the MCMC diagnostics for the models using different priors.

Table 2: MCMC Diagnostics for Different Priors

Prior	Mean ESS	Mean R-hat
Half-Cauchy	4976.061	0.9998
Gamma	6818.535	0.9997
Product Half-Cauchy	3000.933	1.0010
Weibull	6630.414	0.9998
Reciprocal-Gaussian	5551.344	0.9998
Inverse-Gamma	5953.725	0.9998

The mean R-hat values across all models are close to 1.0, indicating good convergence of the MCMC chains. However, the Product Half-Cauchy prior has a lower mean ESS compared to the other priors, suggesting that while the chain has converged, the sampling efficiency is reduced. This could be due to higher auto-correlation in the samples, which warrants further investigation.

9.3 Posterior Predictive Checks

Posterior predictive checks (PPCs) are used to assess the fit of the models by comparing the observed data with data simulated from the posterior distribution. The goal is to evaluate whether the model is capable of generating data that looks similar to the observed data.

Figure 6 shows the posterior predictive densities for models using different prior distributions, overlaid on the observed data (black dashed line). Each colored line represents the predictive density generated by a model using a different prior. The plot demonstrates that most of the priors result in posterior predictive distributions that closely follow the observed data, as indicated by the overlap between the colored lines and the black dashed line. The Gamma prior, represented by the red line, shows a slight deviation at lower values, which might indicate that this model is somewhat over-fitting or under-fitting in this region. The other priors (Half-Cauchy, Inverse-Gamma, Product Half-Cauchy, Reciprocal-Gaussian, and Weibull) show predictive densities that are very similar to each other and closely match the observed data, suggesting that these models fit the data well.

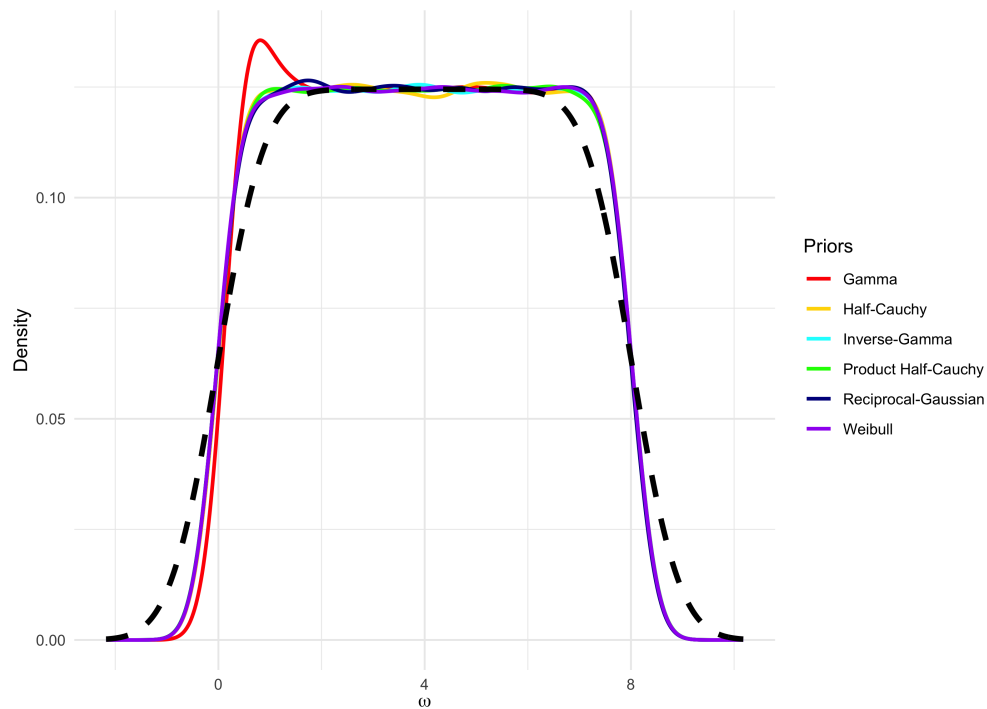


Figure 6: Posterior predictive densities for different priors

References

- ANDRADE, JOSÉ AILTON ALENCAR AND O’HAGAN, ANTHONY. (2006). Bayesian robustness modeling using regularly varying distributions. *Bayesian Analysis* **1**(1), 169–188.
- ANDRADE, JOSÉ AILTON ALENCAR AND O’HAGAN, ANTHONY. (2011). Bayesian robustness modelling of location and scale parameters. *Scandinavian Journal of Statistics* **38**(4), 691–711.
- ANGERS, JEAN-FRANCOIS. (2000). P-credence and outliers. *Metron - International Journal of Statistics* **0**(3-4), 81–108.
- ASTRAATMADJA, TRI L. AND BAILER-JONES, CORYN A. L. (2016, November). Estimating distances from parallaxes. ii. performance of bayesian distance estimators on a gaia-like catalogue. *The Astrophysical Journal* **832**(2), 137.
- BAILER-JONES, CORYN A. L. (2015, oct). Estimating distances from parallaxes. *Publications of the Astronomical Society of the Pacific* **127**(956), 994–1009.
- BAILER-JONES, C. A. L., RYBIZKI, J., FOUESNEAU, M., DEMLEITNER, M. AND ANDRAE, R. (2021, February). Estimating distances from parallaxes. v. geometric and photogeometric distances to 1.47 billion stars in gaia early data release 3. *The Astronomical Journal* **161**(3), 147.
- BARNDORFF-NIELSEN, O. E., KENT, JOHN T. AND SØRENSEN, MICHAEL. (1982). Normal variance-mean mixtures and z distributions. *International Statistical Review* **50**, 145–159.

- BHADRA, ANINDYA, DATTA, JYOTISHKA, POLSON, NICHOLAS G AND WILLARD, BRANDON. (2015). The horseshoe+ estimator of ultra-sparse signals. *arXiv preprint arXiv:1502.00560*.
- BHADRA, ANINDYA, DATTA, JYOTISHKA, POLSON, NICHOLAS G AND WILLARD, BRANDON T. (2019). Lasso meets horseshoe: A survey. *Statistical Science*. forthcoming.
- BROWNE, WILLIAM J. AND DRAPER, DAVID. (2006). A comparison of Bayesian and likelihood-based methods for fitting multilevel models. *Bayesian Analysis* **1**(3), 473 – 514.
- CARPENTER, BOB, GELMAN, ANDREW, HOFFMAN, MATTHEW D, LEE, DANIEL, GOODRICH, BEN, BETANCOURT, MICHAEL, BRUBAKER, MARCUS A, GUO, JIQIANG, LI, PETER AND RIDDELL, ALLEN. (2017). Stan: A probabilistic programming language. *Journal of statistical software* **76**.
- CARVALHO, CARLOS M, POLSON, NICHOLAS G AND SCOTT, JAMES G. (2010). The horseshoe estimator for sparse signals. *Biometrika* **97**, 465–480.
- DAWID, A PHILIP. (1973). Posterior expectations for large observations. *Biometrika* **60**(3), 664–667.
- DAWID, A. P., STONE, M. AND ZIDEK, J. V. (1973). Marginalization paradoxes in Bayesian and structural inference (with discussion). *Journal of the Royal Statistical Society: Series B (Statistical Methodology)* **35**, 189–233.
- DE BRUIJNE, J. H. J. (2012, September). Science performance of Gaia, ESA’s space-astrometry mission. *Astrophysics and Space Science* **341**(1), 31–41.
- DE FINETTI, BRUNO. (1961). The Bayesian approach to the rejection of outliers. In: Neyman, Jerzy (editor), *Proceedings of the Fourth Berkeley Symposium on Mathematical Statistics and Probability, Volume 1: Contributions to the Theory of Statistics*. Berkeley: University of California Press. pp. 199–210.
- DESGAGNÉ, ALAIN AND ANGERS, JEAN-FRANCOIS. (2007, 02). Conflicting information and location parameter inference. *Metron - International Journal of Statistics* **LXV**, 67–97.
- FERNIE, JD. (1975). The historical search for stellar parallax. *Journal of the Royal Astronomical Society of Canada, Vol. 69, p. 222* **69**, 222.
- GELMAN, ANDREW. (2006a). Prior distributions for variance parameters in hierarchical models (comment on article by Browne and Draper). *Bayesian Analysis* **1**(3), 515–533.
- GELMAN, ANDREW. (2006b). Prior distributions for variance parameters in hierarchical models (comment on article by Browne and Draper). *Bayesian Analysis* **1**(3), 515 – 534.
- GELMAN, ANDREW, HWANG, JESSICA AND VEHTARI, AKI. (2014). Understanding predictive information criteria for bayesian models. *Statistics and computing* **24**(6), 997–1016.
- GELMAN, ANDREW AND RUBIN, DONALD B. (1992). Inference from Iterative Simulation Using Multiple Sequences. *Statistical Science* **7**(4), 457 – 472.
- GEYER, CHARLES J. (1992, November). Practical markov chain monte carlo. *Statistical Science* **7**(4), 473–483.

- HARTIGAN, J. A. (1998). The maximum likelihood prior. *The Annals of Statistics* **26**(6), 2083 – 2103.
- HOFFMAN, MATTHEW D. AND GELMAN, ANDREW. (2011). The no-u-turn sampler: Adaptively setting path lengths in hamiltonian monte carlo.
- HÜRLIMANN, WERNER. (2011, 01). Transformation invariant distributions and families: the reciprocal and threshold property. *Pioneer Journal of Theoretical and Applied Statistics* **1**, 113–144.
- IBRAHIM, JOSEPH G., CHEN, MING-HUI AND SINHA, DEBAJYOTI. (2005). *Bayesian Survival Analysis*. John Wiley and Sons, Ltd.
- JEFFREYS, HAROLD AND SWIRLES, BERTHA. (1972). *Methods of Mathematical Physics*, 3 edition. Cambridge: Cambridge university press.
- KUH, EDWIN AND MEYER, JOHN R. (1955). Correlation and regression estimates when the data are ratios. *Econometrica* **23**(4), 400–416.
- LINDLEY, D. V. (1968). The choice of variables in multiple regression. *Journal of the Royal Statistical Society: Series B (Statistical Methodology)* **30**, 31–66.
- MENG, XIAO-LI AND ZASLAVSKY, ALAN M. (2002). Single observation unbiased priors. *The Annals of Statistics* **30**(5), 1345 – 1375.
- MIKOSCH, THOMAS. (1999). *Regular variation, subexponentiality and their applications in probability theory*. Eindhoven University of Technology.
- O’HAGAN, A. (1979). On outlier rejection phenomena in Bayes inference. *Journal of the Royal Statistical Society: Series B (Statistical Methodology)* **41**(3), 358–367.
- O’HAGAN, A. (1990). Outliers and credence for location parameter inference. *Journal of the American Statistical Association* **85**(409), 172–176.
- O’HAGAN, ANTHONY AND PERICCHI, LUIS R. (2012). Bayesian heavy-tailed models and conflict resolution: A review. *Brazilian Journal of Probability and Statistics* **26**(4), 372–401.
- POLSON, NICHOLAS G. AND SCOTT, JAMES G. (2012). On the Half-Cauchy Prior for a Global Scale Parameter. *Bayesian Analysis* **7**(4), 887 – 902.
- REID, MARK J. AND MENTEN, KARL M. (2020). The first stellar parallaxes revisited. *Astronomische Nachrichten* **341**(9), 860–869.
- ROBERT, CHRISTIAN. (2016, 7). the curious incident of the inverse of the mean.
- SPOTO, F., TANGA, P., BOUQUILLON, S., DESMARS, J., HESTROFFER, D., MIGNARD, F., ALTMANN, M., HERALD, D., MARCHANT, J., BARACHE, C., CARLUCCI, T., LISTER, T. *and others*. (2017). Ground-based astrometry calibrated by gaia dr1: new perspectives in asteroid orbit determination. *A&A* **607**, A21.

ZELLNER, ARNOLD. (1978). Estimation of functions of population means and regression coefficients including structural coefficients: A minimum expected loss (melo) approach. *Journal of Econometrics* **8**(2), 127–158.

ZELLNER, ARNOLD AND PARK, SOO-BIN. (1979). Minimum expected loss (melo) estimators for functions of parameters and structural coefficients of econometric models. *Journal of the American Statistical Association* **74**(365), 185–193.